

Low-energy interband transitions in $\text{YBa}_2\text{Cu}_3\text{O}_7$

I. I. Mazin, S. N. Rashkeev, A. I. Liechtenstein, and O. K. Andersen

Max-Planck-Institut für Festkörperforschung, D-7000 Stuttgart 80, Federal Republic of Germany

(Received 13 July 1992)

Based on a numerically highly accurate local-density-approximation (LDA) calculation, we present a $\mathbf{k}\cdot\mathbf{p}$ analysis of the interband optical absorption in $\text{YBa}_2\text{Cu}_3\text{O}_7$ in the infrared region ($\hbar\omega < 0.1$ eV). It is shown that the LDA band structure gives rise to three infrared interband transitions: A sharp peak for the in-plane ($E \perp c$) polarization at about 320 cm^{-1} , a wide maximum for $E\parallel c$ at about 420 cm^{-1} , and a structureless absorption ($\epsilon_2 \approx \text{const}$) for $E\parallel c$. The first feature is due to transitions between the apical-oxygen-derived bands, the second one to that between the z -even and z -odd CuO_2 plane bands, and the third one to the transitions between the chain band and the z -odd plane band. The possibility of observing these features in experiment is discussed.

In recent years, the low-energy excitation spectra of the high-temperature superconductors have attracted great interest. It seems that the shape of the Fermi surface^{1,2} (FS) in $\text{YBa}_2\text{Cu}_3\text{O}_7$ is quite accurately described by conventional *ab initio* band-structure calculations³⁻⁵ using the local approximation to density functional formalism (LDA), and that the 1–10 eV optical spectra are also given reasonably well by such an approach.⁶ It is not clear, however, whether the LDA band structure, i.e., the Kohn-Sham eigenvalues, bear any resemblance to the infrared electronic excitations, whose energy is less than 0.1 eV. We know, for instance, that in heavy-fermion systems, the LDA yields correct Fermi surfaces, but much too high electron velocities. It was shown recently⁷ that the experimental Landau damping threshold for the Raman-active phonons in $\text{YBa}_2\text{Cu}_3\text{O}_7$ coincides with the LDA prediction,⁸ thus indicating that the maximum Fermi velocity is essentially the one given by the LDA. However, the question of interband excitations with energy less than 0.1 eV (which are especially important for the superconductivity) is still open. This question was partially addressed before,⁶ however, in order to draw meaningful conclusions for such low energies one needs to know the band structure on a level of accuracy of a few meV. No optical calculation has been performed up to now with the needed accuracy.

In this paper we shall use the presently most accurate LDA calculation to clarify which features in the interband electronic absorption the LDA predicts in the far-infrared region, and compare these predictions with available experimental data.

I. LDA BAND STRUCTURE

Our analysis is based on the full-potential linear-muffin-tin-orbital (LMTO) band structure⁴ of which relevant parts are shown in Fig. 1. As regards the low-energy details, it differs somewhat from the linearized augmented plane-waves band structures⁹ published prior to 1990, but those published after⁵ agree with it. In the

Brillouin zone, there are three regions where two bands near the Fermi level come sufficiently close to produce interband transitions at far-infrared energies: The first region is near the SR line, $\mathbf{k} = (\pi/a, \pi/b, k_z)$, where two parabolic bands come up to the Fermi level, and the higher one crosses it, giving rise to the so-called “stick” sheet.³ The bands near the SR line have wave functions which are predominantly located at the apical oxygen $\text{O}(4)$, as has been described in detail elsewhere.³ The upper band has $\text{O}(4)$ p_y character, with some $\text{Ba } p_x$, $\text{Cu}(1)$

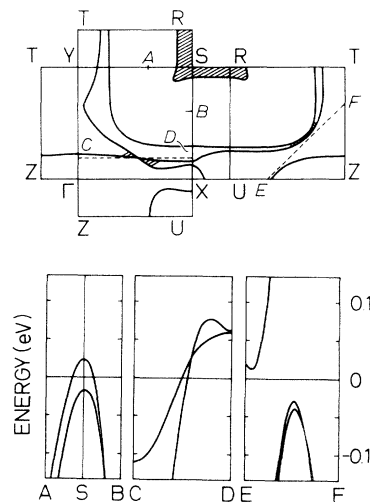


FIG. 1. The LDA Fermi surface and selected parts of the low-energy band structure of $\text{YBa}_2\text{Cu}_3\text{O}_7$, as calculated with the full-potential LMTO method. The cross-hatched regions contribute to the infrared absorption for wave numbers less than about 500 cm^{-1} . Of the bands shown along ASB , the upper one is the $\text{O}(4)$ p_y band and the lower one is the $\text{O}(4)$ p_x band. Along the CD line, the steeper band is the odd plane band, and the less steep band is chainlike near C and even-plane-like near D . Along EF , the highest band is odd-plane-like near E and thereafter chainlike, whereas one of the two lower, nearly degenerate bands is chainlike near E and odd-plane-like near F . The third band is the even plane band.

d_{yz} , and $O(1)$ p_z admixture, and the lower band has $O(4)$ p_x character, with Ba p_y and $\text{Cu}(1)$ d_{xz} admixture. Both have negligible z dispersion. Here, and in the following, x and y are parallel to z , respectively, the a and b axis of the crystal and the chains run in the y direction. It can be shown that the optical matrix elements vanish by symmetry at the S point, but increase linearly away from it. More specifically, the matrix element for light polarized parallel to x is $P_x = \eta_x |k_y - \pi/b|$, and $P_y = \eta_y |k_x - \pi/a|$, where parameters η will be defined below in Sec. II. The distance between the two bands is 40–45 meV, so one expects an interband transition at 320–360 cm^{-1} for in-plane polarization ($E \perp c$).

The second region is near the point $\mathbf{k} = (0.5\pi/a, 0.2\pi/b, 0)$ in the ΓXSY plane, where the “chain” band crosses the upper of the two “plane” bands at the Fermi level. The wave functions of this upper plane band are odd with respect to reflection ($z \rightarrow -z$) in the yttrium plane. Since the orbitals of the chain band are even with respect to reflections in the plane of the chains, which is also perpendicular to the z axis, it is obvious that for $k_z = 0$, the chain band does *not* hybridize with the odd (upper) plane band, but only with the even (lower) plane band. For $k_z = \pi/c$, i.e., in the $ZURT$ plane, the situation is reversed: the chain band does not hybridize with the even (lower), but only with the odd (higher) plane band. This is the reason why there is no crossing between chain and plane bands for $k_z \neq 0$. It is also the reason why the above-lying chain band near $k_z = 0$ pushes the lower (even) plane band *down* and, hence, the two plane bands *apart*, whereas near $k_z = \pi/c$, it pushes the upper (odd) plane band *down* and, hence, the plane bands *together*. For the transitions near $(0.5\pi/a, 0.2\pi/b, 0)$, between the crossing chain and odd plane bands, the interband optical matrix element is nonzero only for z polarization ($E \parallel c$). Such a situation is common in transition metals and was discussed in detail in Ref. 10 where it was shown that the interband conductivity increases linearly with frequency, or equivalently, $\epsilon_2(\omega) \rightarrow \text{const}$, as $\omega \rightarrow 0$. Formally, therefore, the interband transitions start at $\omega = 0$ (as long as we neglect the spin-orbit coupling, which is justified for all transitions considered here).

The third region of low-energy transitions is where the two plane sheets of the FS come close together, i.e., near the point $\mathbf{k} = (0.3\pi/a, 0.3\pi/b, \pi/c)$. Had there been no hybridization between the chain band and the upper (odd) plane band, the intersection of the latter FS sheet with the $k_z = \pi/c$ plane would be similar to its intersection with the $k_z = 0$ plane where the hybridization is forbidden by symmetry, that is, the intersection would be close to the line EF in Fig. 1. Now, due to the hybridization with the chain band, the upper, odd plane band becomes nearly degenerate with the lower, even and non-hybridizing plane band along EF , as seen at the bottom

of the figure. The corresponding far-infrared transitions are active for z polarization, because of different parity, and may be also described as a polarization of the z -directed $\text{Cu}(2)$ - $\text{O}(4)$ - $\text{Cu}(1)$ - $\text{O}(4)$ - $\text{Cu}(2)$ complexes. The energy distance between the two bands varies as a function of \mathbf{k} , so that the corresponding absorption spectrum has a complicated profile, but the low-energy part of this spectrum is dominated by the behavior of the two bands in the $k_z = \pi/c$ plane where, as we have seen, a curve of degeneracy exists close to the line EF . Such a case was not considered in Ref. 10, but it was shown that in the similar case of a degeneracy point near the Fermi surface, a maximum appears in $\epsilon_2(\omega)$, whose energy position and intensity depend on the distance from the degeneracy point to the Fermi level and on how the degeneracy is lifted away from this point. In addition, there will be an increase of ϵ_2 above 700 cm^{-1} , mostly because of the existence of a large region around $((0.3 - 1.0)\pi/a, 0.3\pi/b, \pi/c)$ where two plane bands are nearly parallel and the energy difference is about 900 cm^{-1} . Unfortunately, the $\mathbf{k}\cdot\mathbf{p}$ expansion that we use in the next section to find the optical matrix elements, is not applicable in this energy range, so we had to limit ourselves by the energies less than 700 cm^{-1} .

II. DIELECTRIC FUNCTION IN THE SMALL FREQUENCY LIMIT

The tetrahedron method, which is normally used to perform the Brillouin zone summations in *ab initio* calculations for metals, is based on a piecewise linear interpolation of each band, defined in the order of increasing energy. Near band crossings, this method converges poorly and our experience for elemental transition metals¹⁰ indicates that the mesh size which would be needed in order to obtain a good representation of $\epsilon_2(\omega)$ in the far-infrared region for $\text{YBa}_2\text{Cu}_3\text{O}_7$ is unattainable. We have therefore used $\mathbf{k}\cdot\mathbf{p}$ -perturbation theory to fit the *ab initio* band structure near the degeneracy points or lines, and then calculated $\epsilon_2(\omega)$ analytically. This method has the equally important advantage that the optical matrix elements are readily obtained as parameters of the $\mathbf{k}\cdot\mathbf{p}$ expansion. The fits were performed on a mesh with the step $\delta k \approx 0.05 \text{ \AA}^{-1}$ around the degeneracies and the parameter values are shown in Table I. We now specify the $\mathbf{k}\cdot\mathbf{p}$ Hamiltonians taking the zero of energy at the Fermi level.

The $O(4)$ p_y and $O(4)$ p_x bands near the SR line are well represented by the eigenvalues of the Hamiltonian,

$$H^{O(4)-O(4)}(\mathbf{k}) = \begin{pmatrix} -\mu_{1x}k_x^2 - \mu_{1y}k_y^2 - \Delta_1 & \eta k_x k_y \\ \eta k_x k_y & -\mu_{2x}k_x^2 - \mu_{2y}k_y^2 + \Delta_2 \end{pmatrix}$$

TABLE I. Parameters of the $\mathbf{k}\cdot\mathbf{p}$ -perturbation Hamiltonians, atomic units, besides Δ 's, which are in cm^{-1} .

Plane-chain		P	$ v_e - v_o $	Plane-plane		μ	P	O(4)-O(4)		η	Δ_1	Δ_2
v_p	v_c			α	Δ			μ_1	μ_2			
(0.035,0.040)	(0.010,0.102)	0.062	0.140	3.2	460	0.54	0.034	(0.36,0.39)	(0.32,0.58)	0.63	50	280

with $\eta_x \approx \eta_y \equiv \eta$. This gives a narrow peak in ϵ_2^{xx} and in ϵ_2^{yy} around 330 cm^{-1} , whose width is of no physical meaning, since it is less than the interband relaxation frequency. What is of physical meaning is the oscillator strength of this transition, which appears to be about 1.5×10^{-4} electrons. We show this peak convoluted with a Lorentzian of width 20 cm^{-1} in the upper part of Fig. 2.

For the chain-to-odd-plane transition near $\mathbf{k} = (0.5\pi/a, 0.2\pi/b, 0)$, the momentum matrix element P differs from zero only for z polarization, so the $\mathbf{k}\cdot\mathbf{p}$ -perturbation Hamiltonian is

$$H^{c-p}(\mathbf{k}) = \begin{pmatrix} (\mathbf{k} \cdot \mathbf{v}_c) & (k_z P) \\ (k_z P) & (\mathbf{k} \cdot \mathbf{v}_p) \end{pmatrix},$$

where $\mathbf{k} \equiv (k_x, k_y)$ and $\mathbf{v}_i \equiv (v_{ix}, v_{iy})$ with i indicating chain (c) or plane (p). This 2×2 problem can be easily solved and yields the following result for $\epsilon_2^{zz}(\omega)$:

$$\epsilon_2^{zz}(\omega) = 2P/|(\mathbf{v}_p - \mathbf{v}_c) \times (\mathbf{v}_p + \mathbf{v}_c)| + o(\omega).$$

With the fitted parameters (Table I), this gives $\epsilon_2^{zz}(\omega) = 21 + o(\omega)$ and is shown as the constant contribution in the lower part of Fig. 2.

The case of the plane-to-plane transition is more complicated but we were able to fit the band structure in the region of interest by the following $\mathbf{k}\cdot\mathbf{p}$ Hamiltonian:

$$H^{p-p}(\mathbf{k}) = \begin{pmatrix} (k_\eta v_e - \mu k_\xi^2 - \Delta) & (k_z P) \\ (k_z P) & (k_\eta v_o - \mu k_\xi^2 - \Delta) \end{pmatrix},$$

$$\epsilon_2^{zz}(\omega) = \frac{P}{\pi|v_e - v_o|} \sqrt{\frac{2\alpha}{\mu\omega}} \times \begin{cases} F[(2\Delta - \omega)/\alpha\omega], \\ F[(2\Delta - \omega)/\alpha\omega] - F[(2\Delta + \omega)/\alpha\omega], \end{cases} \text{ for } \begin{cases} 2\Delta/(\alpha + 1) < \omega < 2\Delta/(\alpha - 1) \\ 2\Delta/(\alpha - 1) < \omega \end{cases}$$

and zero otherwise. Here, $\alpha = |v_e + v_o|/|v_e - v_o|$, and $F(x) = \int_x^1 \sqrt{t-x}/\sqrt{1-x^2} dt$. With the parameter values from Table I, we obtain the contribution shown in Fig. 2 on top of the 21 from the chain-plane transitions.

III. EXPERIMENTAL SITUATION

As a result of our analysis of the LDA band structure, we predict three interband features in the electronic absorption for wave numbers less than 800 cm^{-1} . It seems to be difficult to observe such features, first of all because of the strong Drude absorption, and also because of the presence of other absorption mechanisms, such as optical phonons, but we find it encouraging that the experimentalists always see a wiggle in the $\epsilon_2(\omega)$ curves at about 350 cm^{-1} .¹¹⁻¹⁶ In the experimental papers, this feature is often interpreted as an infrared phonon. There are two arguments against such an interpretation: First, this feature seems to be too strong for an ordinary phonon. Second, in a single-domain measurement,¹⁴ the position of the peak is exactly the same for x and y polarization. Furthermore, recent measurements¹⁷ on isotope-substituted samples show *no* isotope shift for this peak,

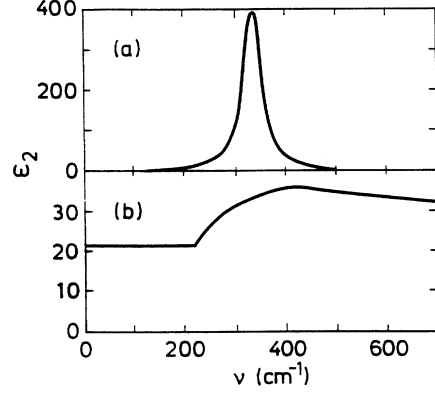


FIG. 2. Calculated interband contributions to $\epsilon_2(\omega)$ in $\text{YBa}_2\text{Cu}_3\text{O}_7$. The upper panel (a) shows $\epsilon_2^{xx} \approx \epsilon_2^{yy}$ and is contributed by the $O(4) p_x$ - $O(4) p_y$ transitions near the SR line. The lower panel (b) shows ϵ_2^{zz} and is contributed by the chain-plane ($\epsilon_2^{zz} = 21$) and plane-plane transitions.

where the ξ axis is in the $[110]$ direction, the η axis in the $[-1,1,0]$ direction, and the origin is at $(0.34\pi/a, 0.34\pi/b, \pi/c)$. Here e (o) stand for the even (odd) bands. P is the momentum matrix element for zz polarization, and the elements for xx and yy polarization are neglected. The solution for ϵ_2 is

while others experience considerable isotope effect.

There are nearly no measurements of the optical absorption parallel to the z axis. The only one we know of is the above-mentioned experiment¹⁷ on the isotope-substituted samples. In this experiment a peak of a complicated shape is observed near 570 cm^{-1} , which may be represented as a superposition of a isotope-sensitive, phononlike feature and an isotope-insensitive peak presumably of electronic origin. This peak is weaker and also narrower than what calculations predict, but nevertheless could be identified with our “plane-plane” transition. Our chain-plane transition is structureless and therefore hardly detectable.

IV. CONCLUSIONS

Based on numerically accurate LDA energy bands, we have presented a $\mathbf{k}\cdot\mathbf{p}$ analysis of the far-infrared optical absorption of $\text{YBa}_2\text{Cu}_3\text{O}_7$. We have found that there are three interband electronic transitions in the infrared region. One is active for in-plane polarization ($E \perp c$) and is caused by $O(4) p_x$ - $O(4) p_y$ transitions near the SR line. The two others are active for $E \parallel c$ and are caused by chain-plane and plane-plane transitions. The first transition gives a sharp peak at about 320 cm^{-1} , which seems

to be seen in several experiments. The second one gives a constant term in the imaginary part of the dielectric function and is probably not detectable by reflectivity measurements. The last transition gives a broad maximum around 420 cm^{-1} and this feature might have been observed.

ACKNOWLEDGMENTS

We want to thank Dr. A. V. Bazhenov for many stimulating discussions and for making the results of his optical experiments on isotope-substituted samples available to us prior to publication.

- ¹J.G. Tobin, C.G. Olson, C. Gu, J.Z. Liu, F.R. Solal, M.J. Fluss, R.H. Howell, J.C. O'Brien, H.B. Radousky, and P.A. Sterne, *Phys. Rev. B* **45**, 5563 (1992).
- ²C.M. Fowler, B.L. Freeman, W.L. Hulst, J.C. King, F.M. Mueller, and J.L. Smith, *Phys. Rev. Lett.* **68**, 534 (1992); **68**, 3937 (1992).
- ³I.I. Mazin, O. Jepsen, A.I. Liechtenstein, O.K. Andersen, S.N. Rashkeev, and Y.A. Uspenski, *Phys. Rev. B* **45**, 5103 (1992); *Phys. Rev. Lett.* **68**, 3936 (1992).
- ⁴C.O. Rodriguez, A.I. Liechtenstein, I.I. Mazin, O. Jepsen, O.K. Andersen, and M. Methfessel, *Phys. Rev. B* **42**, 2692 (1990); O.K. Andersen, A.I. Liechtenstein, C.O. Rodriguez, I.I. Mazin, O. Jepsen, V.P. Antropov, O. Gunnarsson, and S. Gopalan, *Physica C* **185-189**, 147 (1991); I.I. Mazin, O.K. Andersen, A.I. Liechtenstein, O. Jepsen, V.P. Antropov, S.N. Rashkeev, V.I. Anisimov, J. Zaanen, R.O. Rodriguez, and M. Methfessel, in *Proceedings of the Conference on Lattice Effects in High-Temperature Superconductors, Santa Fe, 1992* (World Scientific, Singapore, in press).
- ⁵W.E. Pickett, R.E. Cohen, and H. Krakauer, *Phys. Rev. B* **42**, 8764 (1990).
- ⁶E.G. Maksimov, S.N. Rashkeev, S.Y. Savrasov, and Y.A. Uspenski, *Phys. Rev. Lett.* **63**, 1880 (1989); E.T. Heyen, S.N. Rashkeev, I. Mazin, O.K. Andersen, R. Liu, M. Cardona, and O. Jepsen, *Phys. Rev. Lett.* **65**, 3048 (1990); S. Gopalan, J. Kircher, O.K. Andersen, O. Jepsen, M. Alouani, and M. Cardona, *Physica C* **185-189**, 1473 (1991); H. Chen, J. Callaway, N.E. Brener, and Z. Zou, *Phys. Rev. B* **43**, 383 (1991).
- ⁷B. Friedl, C. Thomsen, H.-U. Habermeier, and M. Cardona, *Solid State Commun.* **81**, 989 (1992).
- ⁸O. Jepsen, I.I. Mazin, O.K. Andersen, A.I. Liechtenstein, and C.O. Rodriguez (unpublished).
- ⁹W.E. Pickett, *Rev. Mod. Phys.* **61**, 433 (1989).
- ¹⁰S.N. Rashkeev, Yu.A. Uspenski, and I.I. Mazin, *Zh. Eksp. Teor. Fiz.* **88**, 1687 (1985) [*Sov. Phys. JETP* **61**, 1004 (1985)].
- ¹¹R.T. Collins, Z. Schlesinger, F. Holtzberg, C. Field, U. Welp, G.W. Crabtree, J.Z. Liu, and Y. Fang, *Phys. Rev. B* **43**, 8701 (1991).
- ¹²K. Kamaras, S.L. Herr, C.D. Porter, N. Tache, D.B. Tanner, S. Etemad, T. Venkatesan, E. Chase, A. Inam, X.D. Wu, M.S. Hegde, and B. Dutta, *Phys. Rev. Lett.* **64**, 84 (1990).
- ¹³K.F. Renk, B. Gorshunov, J. Schutzmann, A. Pruckl, B. Brunner, J. Betz, S. Orbach, M. Klein, G. Muller, and H. Piel, *Europhys. Lett.* **15**, 661 (1991).
- ¹⁴T. Pham, M.W. Lee, H.D. Drew, U. Welp, and Y. Fang, *Phys. Rev. B* **44**, 5377 (1991).
- ¹⁵T. Timusk, C.D. Porter, and D.B. Tanner, *Phys. Rev. Lett.* **66**, 663 (1991).
- ¹⁶F. Gao, G.L. Carr, C.D. Porter, D.B. Tanner, S. Etemad, T. Venkatesan, A. Inam, B. Dutta, X.D. Wu, G.P. Williams, and C.J. Hirschmugl, *Phys. Rev. B* **43**, 10383 (1991).
- ¹⁷A.V. Bazhenov and K.B. Rezhchikov, *Physica C* **192**, 411 (1992); and (unpublished).